MSc in Photonics

PHOTONICS**BCN**

Universitat Politècnica de Catalunya (UPC)
Universitat Autònoma de Barcelona (UAB)
Universitat de Barcelona (UB)
Institut de Ciències Fotòniques (ICFO)

http://www.photonicsbcn.eu

Master in Photonics

MASTER THESIS WORK

Polymer optofluidic systems

Jordi Vila i Planas

Supervised by Dr. Andreu Llobera, (IMB-CNM, CSIC)

Presented on date 9th september 2009

Registered at

Escola Tècnica Superior d'Enginyeria de Telecomunicació de Barcelona

Polymer optofluidic systems

Jordi Vila i Planas

Centre Nacional de Microelectrònica (IMB-CNM, CSIC), Campus UAB s/n, Bellaterra 08193, Spain

E-mail: jordi.vila@imb-cnm.csic.es

Abstract. The cell concentration in cultures is an old topic not solved yet, in order to fix this problem a new technique for cell counting has been implemented. Using a multiple internal reflexion (MIR) device and a white light source we can determine the cell concentration as far as 38.4 ± 0.5 kcell/mL, in other words 53 ± 1 cells, we are also able to recognize between dead and live cells until 6.7 ± 0.3 % of dead cells.

Keywords: Optofluidic, μTAS, Biosensor, cell counter, PDMS

1. Introduction

Huge interest to optical sensing has been devoted due to its high sensitivity, in combination with chemical and microfluidics we have the so called photonic lab on a chip systems. Two main approaches of photonic lab on a chip systems can be found in the literature: performance enhancement, which means the development of High-throughput systems (HTS) for multiparametric detection [1]; or accuracy enhancement, being the most significant example the use of optical tweezers for single cell analysis and manipulation [2]. Due to technological complexity, the low cost assumption is generally not fulfilled in both approaches. Additionally, since the optical manipulation is a serial process, the processing rate is very low. Both the processing rate and the low cost is generally associated with the use of polymers, and specially poly(dimethylsiloxane) (PDMS), using soft lithographic methods [3]. Considering its excellent optical and structural properties, it can be monolithically defined microfluidic and photonic elements. The integration of photonic elements also allows removing the bulky inverted microscope and the external filters [4] from the experimental setup, having hence an in-plane configuration with much higher accessibility. Finally, its biocompatibility and its low cost make of this material the most suitable for meeting the previously mentioned requirements.

Phase and wavelength changes are known to provide with the highest sensitivity. Nevertheless, they are also prone to have more interference from small fluctuations [5] from light sources, temperature, etc. Therefore, Intensity-based photonic lab on a

chip generally is the selected method by many researchers, and examples of such are fluorescence [6], absorbance [7] and scattering [8].

When the particles crosses the light beam, the light-particle interaction allows determining its optical properties [8]. If we use a fluorescent-labeled (FL) cell, one can detect antigen/antibody reactions, enzymatic activity, etc. Nevertheless, the labeling adds an additional step on the cell preparation and fluorescence emits in 4π stereoradians, which causes to have a very small amount of fluorescence light at the detector if it is positioned away from the excitation region. Conversely, absorbance measurements can be done without requiring labeling or with a simpler labeling method.

According to the Beer-lambert law [9], the absorbance is directly proportional to the path length for a fixed concentration. Hence, larger interrogation regions should provide lower limit of detection for a fixed analyte concetration. This issue was already solved in a previous work, where it was demonstrated that defining an air mirror on the vicinity of the photonic lab on a chip substantially improves their performance, resulting in a reduction of the integration time and at the same time an increasing of the SNR, which leaded to a higher sensitivity and a lower LOD, allowing us to define the multiple internal reflexion systems [10].

The MIR structure previously mentioned has been used for two different key magnitudes in cellular analysis: population and life/dead cell ratio. In the first case, a single scattering measurement allows determining the population. When using a marker for death cells, the dead/live ratio can be determined by absorbance.

2. Design

2.1. Optofluidic system design

A schema of the MIR configuration is presented in figure 1. From a fluidic point of view, the MIR systems consist of a fillable interrogation region directly connected to fluidic input/output reservoirs. Optically, they form a complex system with a high degree of monolithic integration, since they comprise self-alignment systems for adequate positioning of optical fibers, lenses and focusing mirrors, which have been designed considering only the refractive indices of PDMS (n=1.41), buffer solution (phosphate buffer, pH 7.4, 10 mM, $n = 1.334$) and air ($n = 1.00$). Firstly, the divergence of the light emerging from the fiber optic is partially corrected through a cylindrical microlens, which has been defined so as to have parallel beams at the first part of the interrogation region. Using such lenses and fixing the optical fibers in its focus results in light emerging from the microlenses with parallel beams in the horizontal direction while it broadens in the vertical axis. This situation is suboptimal, since it would be more desirable to have a cross-section correction. Nevertheless, having a focal point instead of a focal plane could only be obtained with spherical or aspherical microlenses. Such lenses are are either technologically difficult to obtain [11] or require non-standard processing methods [12], with the consequent cost increase, which is opposite to the aim of the

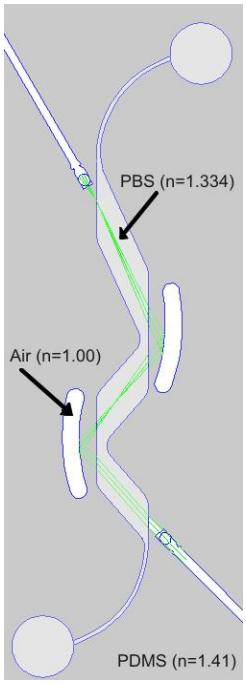

(a) ray tracing simulation for PDMS-PBS-Air used materials.

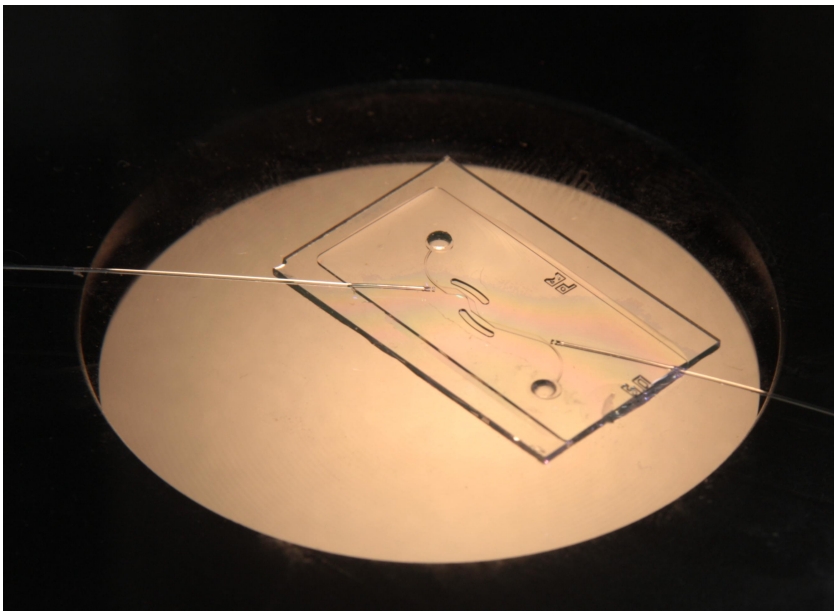

(b) Experimental setup

Figure 1: The photonic lab on a chip system.

present work.

Figure 1(a) also shows the ray tracing propagation inside the MIR system. After crossing the cylindrical microlens, beam divergence is partially corrected, having parallel beams in the horizontal axis. Light is injected in the interrogation region and reaches the PBS-PDMS interface. At this point light is transferred from a media with low RI ($n = 1.334$) to PDMS, which has a higher RI ($n = 1.41$). Hence, most of the light is coupled to the PDMS. When the light reaches the air mirror (air, $n = 1.00$) with the appropriate incidence angle, Total Internal Reflection (TIR) at the PDMS-air layer is obtained, resulting in a complete back reflection of the light towards the PDMS. Considering the refractive indices of the media involved (PDMS and air) and using the Snell's law, the critical propagation angle is $\theta_{cPDMS-air} = 45.17°$. All the propagation angles $\theta > \theta_{cPDMS-air}$ satisfiy the TIR conditions and are reflected back to the PDMS, reaching again the interrogation region. In this back reflection the TIR conditions can be calculated again (considering the RI of PDMS and PBS), being in this case the critical angle $\theta_{cPDMS-PBS} = 70.60°$ The optimal situation is when the propagation angles match the TIR regime at the PDMS-air region, but do not at the PDMS-PBS interface. Otherwise light could remain confined at the PDMS and would not be transferred to the interrogation region. After this first reflection, light is re-injected into the system and reaches the second air mirror, which reflects again the light while focusing it on the vicinity of the collecting optical fibers. Thus, light propagates in

the system following a zig-zag path (green line in figure 1(a)). Hence, with the air mirrors the optical path can now meaningfully lengthened without dramatically decreasing the SNR [13].

2.2. Cell culture and labelling

Human monocytic cell line THP-1 (ECACC No.88081201) was maintained in RPMI 1640 medium (Gibco) with 20% FBS (Gibco) at 37°C in 5% CO_2. For light scattering detection, living cells were rinsed twice in PBS tempered at 37°C. To obtain a cell death population, a simulation was performed, fixing monocytes with 4% paraformaldehyde in PBS for 10 minutes. Immediately, cells were stained with trypan blue in PBS (1 : 1) for 5 minutes and rinsed twice in PBS to ensure good labelling exclusively inside the cells. Both populations were diluted to obtain all the desired concentrations.

3. Fabrication

The production of the device is based on standard soft-lithography.

Focusing on the low cost issue, a cheap 700 μm-thick soda-lime glass is used as a substrate and structures defined with SU-8 photoresist (MicroChem, Corp., Newton, MA, USA) are used as a master. After its cleaning, a dehydratation process has been made at 200 °C for 1 h, a double adhesion promoter layer is applied so as to obtain better mechanical stability and robustness, together with an increase of the durability of the fabricated masters. Afterwards a Cr layer is sputtered. Then we dehydrate the substrate at 150 °C for 1 h before spin an adhesion layer of SU-8 at 3000 rpm for 60 s, obtaining a 4 μm thickness layer. After 10 min drying at 95 °C it is exposed without mask to 75 mJ/cm^2 of UV light and then a post-exposure bake (PEB) of 5 min at 200 °C is made.

Once the adhesion layer has been made, a single spin-on process using SU-8 50 (400 rpm for 30 s) is done, achieving a thickness of 250 μm. After 3 h drying at 95 °C, an exposure of 750 mJ/cm^2 is made. Then the wafer is placed for 20 min at 95 °C.

The last step is to develop the master with propylene glycol methyl ether acetate (PGMEA, MicroChem, Corp., Newton, MA, USA).

The PDMS (Sylgard 184 elastomer kit, Dow Corning, Midland, MI, USA) pre-polymer has been obtained mixing the curing agent with the elastomer base in 1 : 10 ratio (v:v). Controlled volume of this mixture is dispensed over the master and cured for 20 min at 80 °C. Afterwards, the cured PDMS was peeled off from the master and the fluidic ports were opened. Then, both the PDMS and a second sodalime glass substrate were exposed to an oxygen plasma [14] in a barrel etcher (Surface Technology Systems, Newport, UK). Immediately afterwards, both surfaces are brought in contact, causing its irreversible sealing. This covalent bonding between the PDMS and the soda-lime glass ends the fabrication process. Considering the master thickness and the MIR dimensions, the total interrogation volume is 1.43 μL.

4. Experimental Results

4.1. Experimental setup

Light emitted from an broadband light source (Ocean Optics HL-2000, Dunedin, FL, USA) is coupled into a multimode optical fibers with a diameter of 230 μm, which is located inside the self-alignment system and it is pushed until it reaches the constriction. This constriction is located at the position where, in accordance to the RI of the materials, parallel beams are obtained after the microlens. The readout comprises an identical optical fibers, which is also inserted on the output self-alignment system and carries the signal to a spectrometer (Ocean optics HR4000, Dunedin, Fl, USA) with a spectral resolution of 0.2 nm and an integration time of 30 ms. Measurements have been done at room temperature in a temperature-controlled lab.

To avoid non desired cell death and minimize non controlled variations in the optical measurements, all the experimental section was carried out with the minimum required time and keeping the monocytic cell line under culture conditions (37 °C in 5% CO_2) until the measurement.

Figure 1(b) shows the photonic lab on a chip with the optical fibers positioned and ready to be used in accordance to the previously described protocol.

4.2. Live cells: scattering

The absorbance spectra as a function of cell concentration are shown in figure 2(a). As expected, due to the diameter of such cells (between 7 and 15 μm), a nearly flat absorption band can be observed for all cell concentrations (at low and high wavelengths, the decrease of the absorbance is associated to the limitations of the halogen lamp). It can also be seen how an increase of the cell concentration only causes an increase of the maximum absorbance; the spectral behavior of the system remains unchanged.

The most significant difference of the proposed photonic lab on a chip with these previously presented is that instead of measuring the absorbance at a fixed wavelength, with the proposed MIR systems, the whole cell spectral response is obtained in a single measurement which only requires 30 ms. This analysis method allows simultaneous in situ detection of different analytes by choosing the appropriate working wavelengths. Once the spectral response is obtained for different cell concentrations, the absorbance as a function of the cell concentration can also be determined, obtaining the expected linear behavior. Interestingly, the linear fits allow determining the sensitivity and the LOD of the MIR at a fixed wavelength. From them, it is possible to determine which is the working wavelength that provides with higher sensitivity and/or lower LOD, optimizing the response of the photonic lab on a chip.

The results of this optimization for live cells can be seen in figure 2(b), where the sensitivity and the LOD are plotted as a function of the wavelength. From this figure, it can be seen that a plateau of maximal sensitivity is obtained at wavelengths between 580 and 700 nm, which simultaneously corresponds to a LOD minimal, with values

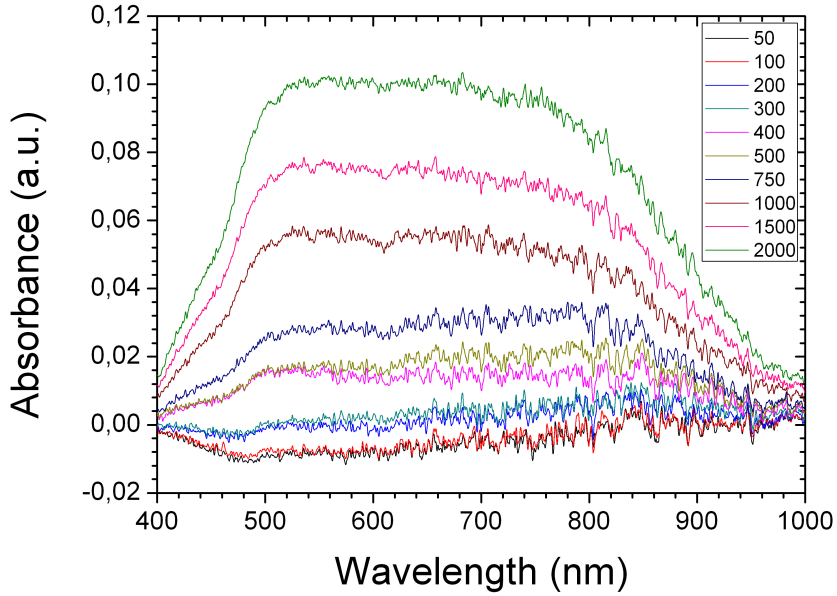

(a) Absorbance spectrum in scattering regime for different cell concentrations, in kcell/mL.

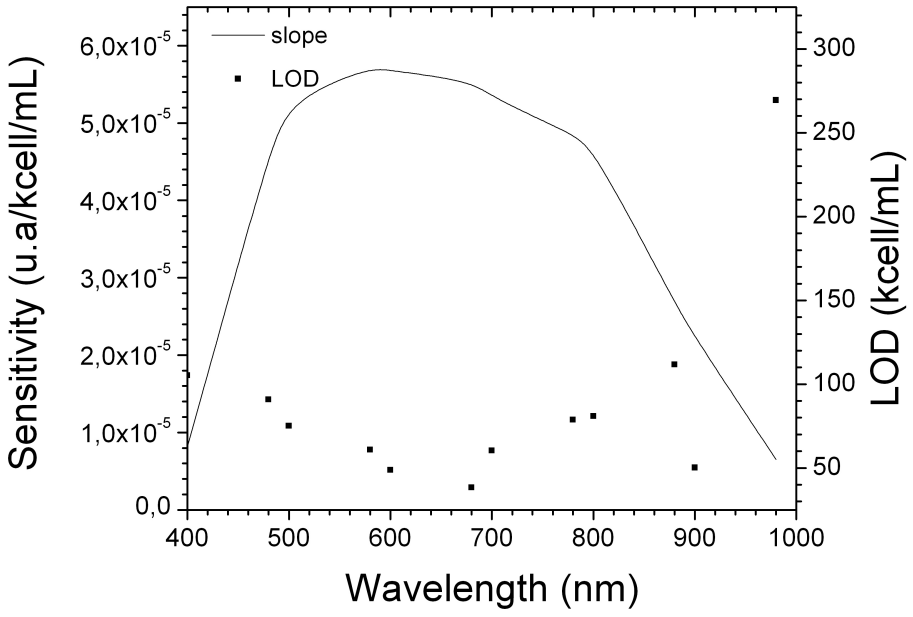

(b) Sensitivity an LOD as function of key wavelengths using different cell concentrations.

Figure 2: Experimental results for scattering working regime.

between 60 ± 1 kcell/mL and 38.4 ± 0.5 kcell/mL. Considering that the system has a volume of $1.43\,\mu$L, these LODs correspond to the detection of 86 ± 1 and 54.9 ± 0.7 cells, respectively.

4.3. Dead cells: scattering+absorption/absorption

When using a vital stain or a dye for cell labelling, two effects simultaneously occur: absorption and scattering. Generally, it is quite challenging to uncouple them, especially if measurements at a single wavelength are done. This issue is addressed and solved with the proposed system: as it is shown in figure 3(a), the absorbance as a function of the wavelength plot for 2000 kcell/mL shows the clear Trypan blue peak at 580 and the scattering band in the wavelength range studied. In section 4.2 it was determined the absorption band for such cell concentration (also shown in figure 2(a) for clarification). Hence, simply by substraction of both spectra, the Trypan blue absorption band can be isolated.

Interestingly, the MIR-based photonic lab on a chip system allows working in three distinct regimes: scattering, scattering+absorbance or absorbance. In the second case, the procedure is identical to that presented in the section 4.2: Several wavelengths have been taken from the reference spectra and the absorbance as a function of the cell concentration has been linearly fitted. The results of these fits are presented in figure 3(b). As expected, due to the strong trypan absorption band, the maximum sensitivity is obtained at $580-600$ nm. At such range, a minimum LOD between 53 ± 1 and 61 ± 1 cells is obtained. It is also noticeable that the scattering band causes to have a significant sensitivity at longer wavelengths, which allows having LODs of some hundred cells in the NIR range. Although such configuration could be interesting for some applications, sometimes it is required to have very high specificity for a given labelled cell. In this case the absorbance measurements are advantageous. The results obtained in the previous section have been taken as reference and subtracted from the spectra, as previously discussed. Again, several key wavelengths have been taken, and their linear fit is shown in figure 3(b). Since only the trypan blue band is obtained, this figure only shows the linear fits of interest, with a minimum LODs of 105 ± 4 cells. The comparison between both methods can also be seen. Although the absorbance method has a slightly smaller sensitivity it provides a much higher specificity since outside the trypan blue region, LODs higher than 350 cells are obtained.

Up to now, we have shown that the proposed photonic lab on a chip is able to work in three different regimes: scattering, scattering+absorption and asorption, obtaining comparable sensitivities and LODs. As a final test, labelled and non-labelled cells are mixed for a fixed concentration, and afterwards injected in the MIR. The idea is to be able to determine the dead/live cell ratio in a single 30 ms measurement. The results of such experiment are presented in the next subsection.

4.4. dead/live ratio measurement

The absorbance as a function of the wavelength for different dead/live cell ratio is presented in figure 4. As it can be observed, the behaviors of such spectra range from scattering without absorption (0% of dead cells) to a very sharp absorption peak (100% of dead cells). In figure 5 can be observed that the values above the 70% of dead cells

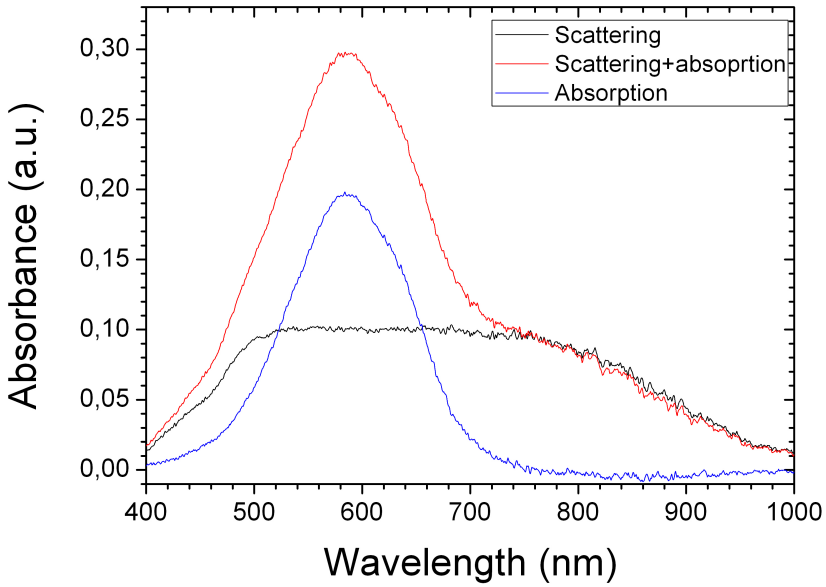

(a) Absorbance spectrum for a cell concentration of 2000 kcell/mL

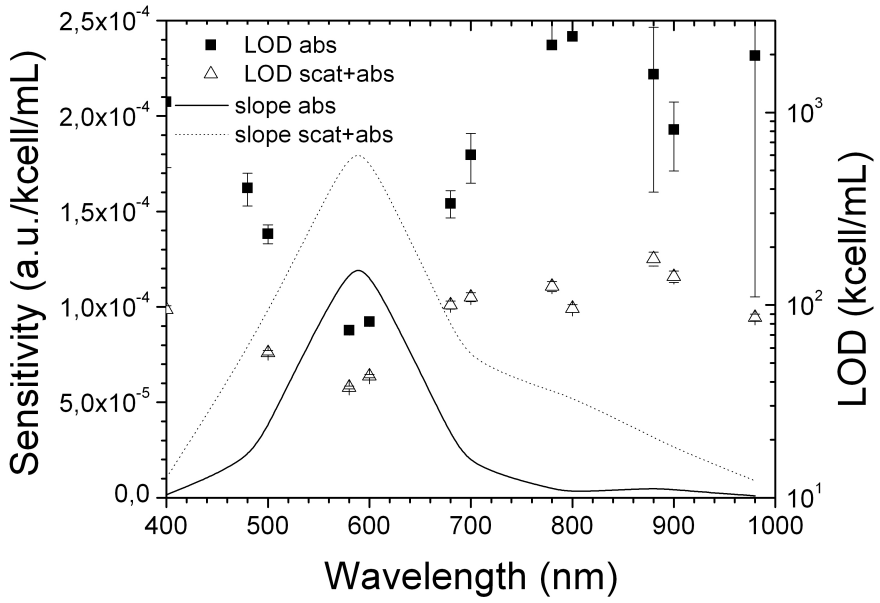

(b) Sensitivity an LOD as function of key wavelengths using different cell concentrations.

Figure 3: Experimental results for absorption and absorption + scattering working regimes.

do not match the tendency. To understand this effect, the same cell dilution was placed in a Neubauer cell counter, and the results of the counted number of cells as a function of the % of dead cells are presented in table 1.

From these data, it can be seen that dilutions above 70% have a significant cell

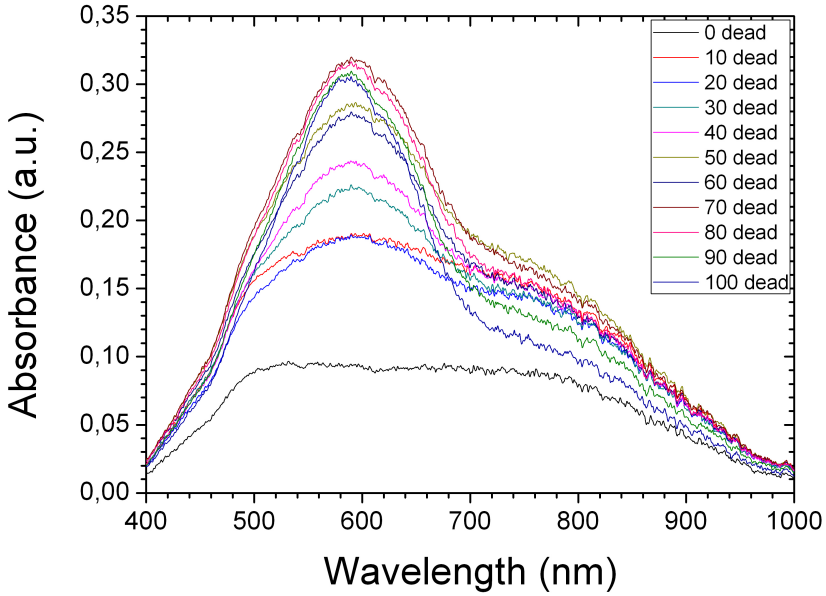

Figure 4: Absorbance spectrum of 2000 kcell/mL for different dead/live ratio in % of dead cells.

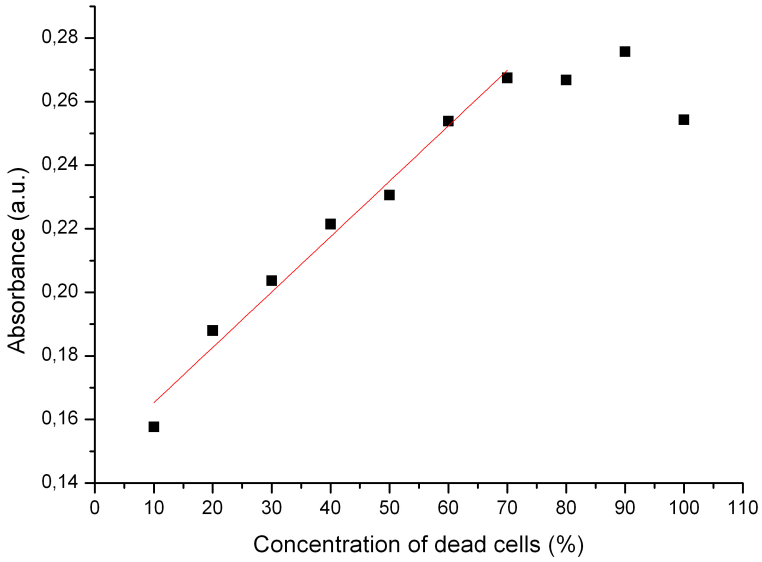

Figure 5: Linear fit of 2000 kcell/mL concentration. Neglecting the last three points the LOD is $7.7 \pm 0.4\%$ of dead cells.

deficit, which explains the unexpected decrease of the absorbance in this range. This point is also noteworthy, since this behavior can be understood as a self-test system: if the experimental value falls outside the calibration curve, a cell deficit is likely to have

Table 1: Dead cell concentration results with a Neubauer method.

	0%	10%	20%	30%	40%	50%	60%	70%	80%	90%	100%
(kcell/mL)	1970	1715	1970	2067	1853	1565	1883	1577	1323	1205	915

happened.

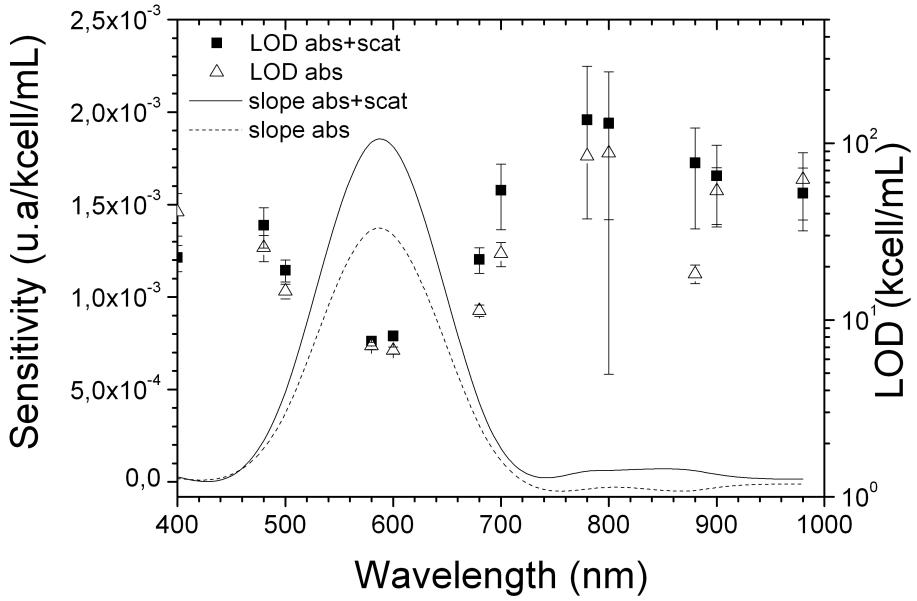

Figure 6: Sensitivity an LOD as function of key wavelengths using different dead/live ratios.

Once it has been clarified the values above the 70%, they have not been used for determining the sensitivity and the LOD. Similar to the previous section, these spectra have been analyzed with two methods; scattering+absorption and absorption. As it can be observed, the highest sensitivity corresponds to the trypan blue region (580-600 nm), decreasing sharply both for longer and shorter wavelengths. Since a fixed cell number (within experimental error) has been used, the scattering band should remain at a fixed value. Variations of this band also provide information regarding how distinct two populations are. Also due to this fixed population, it is clear why when we plot the sensitivity and the LOD as a function of the % of dead cells, no scattering effects are observed and only the wavelengths where the trypan blue absorbs are of interest, having a LOD of 7.7 ± 0.4 % of dead cells.

Due to the constant population level, the absorption measurements are suitable to provide with lower LODs. The procedure has been similar to that previously presented and the results are shown in figure 6. In this case the experimental and statistical errors of the scattering+absorption measurements make difficult to compare their specificity, although the thinner FWHM of the sensitivity for the absorption method may suggest that this protocol has a slightly higher specificity. Again, a decrease of the sensitivity

is obtained, although the LOD for absorption has been experimentally measured to be $6.7 \pm 0.3\,\%$ of dead cells.

5. Conclusions and future work

In this work a photonic lab on a chip has been fabricated with PDMS. The photonic lab on chip has some desirable characteristics such as, low cost, high degree of monolithical integration, standard fabrication technology and biocompatibility.

In order to perform the experiments is not needed to use any expensive benchtop equipment and the complete setup requires just a white light source, optical fibers and an spectrometer. The device is able to act as a cell counter in continuous and can also detect the dead/live ratio. The preparation of the samples to be measured can be made in some minutes in standard concentration, spending just 1.43μL of volume.

The next step will be functionalization of the inner face of the PDMS in order to obtain an integrated bioreactor, allowing expanding the possible applications, such as detection of enzymatic reactions or metabolic activity.

6. Acknowledgements

I am indebted to my supervisor, Dr. Andreu Llobera for his help and encouragement throughout the course of this work. The research leading to these results has received funding from the European Research Council under the European Community's Seventh Framework Programme(FP7/2007-2013) / ERC grant agreement n° 209243.

References

[1] Lin Luan, Randall D. Evans, Nan M. Jokerst, and Richard B. Fair. Integrated optical sensor in a digital microfluidic platform. *IEEE Sensors Journal*, 8:628–635, 2008. 1

[2] Wibke Hellmich, Christoph Pelargus, Kai Leffhalm, Alexandra Ros, and Dario Anselmetti. Single cell manipulation, analytics, and label-free protein detection in microfluidic devices for systems nanobiology. *Electrophoresis*, 26:3689–96, 2005. 1

[3] Younan Xia and George M. Whitesides. Soft lithography. *Angewandte Chemie International Edition*, 37:550–575, 1998. 1

[4] Oliver Hofmann, Xuhua Wang, Alastair Cornwell, Stephen Beecher, Amal Raja, Donal D C Bradley, Andrew J Demello, and John C Demello. Monolithically integrated dye-doped pdms long-pass filters for disposable on-chip fluorescence detection. *Lab on a chip*, 6:981–7, 2006. 1

[5] Y Salvade and R Dandliker. Limitations of interferometry due to the flicker noise of laser diodes. *Journal of the Optical Society of America. A, Optics, image science, and vision*, 17:927–32, 2000. 1

[6] Dominik Greif, Lukas Galla, Alexandra Ros, and Dario Anselmetti. Single cell analysis in full body quartz glass chips with native uv laser-induced fluorescence detection. *Journal of chromatography. A*, 1206:83–8, 2008. 1

[7] Purnendu K. Dasgupta, Zhang Genfa, Simon K. Poruthoor, Steven Caldwell, Shen Dong, and Su-Yi Liu. High-sensitivity gas sensors based on gas-permeable liquid core waveguides and long-path absorbance detection. *Analytical Chemistry*, 70:4661–4669, 1998. 1

[8] Z Wang, J El-Ali, M Engelund, T Gotsaed, I R Perch-Nielsen, K B Mogensen, D Snakenborg, J P Kutter, and a Wolff. Measurements of scattered light on a microchip flow cytometer with integrated polymer based optical elements. *Lab on a chip*, 4:372–7, 2004. 1

[9] Byung-ho Jo, Linda M Van Lerberghe, Kathleen M Motsegood, and David J Beebe. Three-dimensional micro-channel fabrication in polydimethylsiloxane (pdms) elastomer. *Journal of microelectromechanical systems*, 9:76–81, 2000. 1

[10] A Llobera, R Wilke, and S Büttgenbach. Enhancement of the response of poly(dimethylsiloxane) hollow prisms through air mirrors for absorbance-based sensing. *Talanta*, 75:473–479, 2008. 1

[11] GC Firestone and A. Y. Yi. Precision compression molding of glass microlenses and microlens arrays–an experimental study. *Applied Optics*, 44:6115–6112, 2005. 2.1

[12] P Ruther, B Gerlach, J Göttert, M Ilie, J Mohr, A Müller, and C Ossman. Fabrication and characterization of microlenses realized by a modified liga process. *Pure and applied optics*, 6:643–653, 1997. 2.1

[13] A Llobera, S Demming, R Wilke, and S Büttgenbach. Multiple internal reflection poly(dimethylsiloxane) systems for optical sensing. *Lab on a Chip*, pages 1560–1566, 2007. 2.1

[14] TA Gopel. *Sensors: A Comprehensive Survey, Vol. 3, Pt. II, Chemical and Biochemical Sensors*. Wiley-VCH, 1991. 3